

## Kinetic cooperativity of tyrosinase. A general mechanism

Jose Luis Muñoz-Muñoz<sup>1</sup>, Francisco Garcia-Molina<sup>1</sup>, Ramón Varon<sup>2</sup>, Jose Tudela<sup>1</sup>, Francisco Garcia-Cánovas<sup>1</sup>✉ and Jose N. Rodríguez-López<sup>1</sup>

<sup>1</sup>GENZ: Grupo de Investigación Enzimología, Departamento de Bioquímica y Biología Molecular-A, Facultad de Biología, Universidad de Murcia, Espinardo, Murcia, Spain; <sup>2</sup>Departamento de Química-Física, Escuela de Ingenieros Industriales de Albacete, Universidad de Castilla la Mancha, Avda, España s/n. Campus Universitario, Albacete, Spain

**Tyrosinase shows kinetic cooperativity in its action on *o*-diphenols, but not when it acts on monophenols, confirming that the slow step is the hydroxylation of monophenols to *o*-diphenols. This model can be generalised to a wide range of substrates; for example, type  $S_A$  substrates, which give rise to a stable product as the *o*-quinone evolves by means of a first or pseudo first order reaction ( $\alpha$ -methyl dopa, dopa methyl ester, dopamine, 3,4-dihydroxyphenylpropionic acid, 3,4-dihydroxyphenylacetic acid,  $\alpha$ -methyl-tyrosine, tyrosine methyl ester, tyramine, 4-hydroxyphenylpropionic acid and 4-hydroxyphenylacetic acid), type  $S_B$  substrates, which include those whose *o*-quinone evolves with no clear stoichiometry (catechol, 4-methylcatechol, phenol and *p*-cresol) and, lastly, type  $S_C$  substrates, which give rise to stable *o*-quinones (4-*tert*-butylcatechol/4-*tert*-butylphenol).**

**Keywords:** tyrosinase, *o*-diphenols

**Received:** 10 November, 2010; revised: 14 March, 2011; accepted: 04 July, 2011; available on-line: 29 August, 2011

### INTRODUCTION

Tyrosinase (TYR; monophenol monooxygenase, *o*-diphenol:oxygen oxidoreductase; EC 1.14.18.1) has two copper atoms in its active site and is ubiquitously present in biological systems. It has two physiological activities involving molecular oxygen; (a) the *ortho*-hydroxylation of monophenols to *o*-diphenols and (b) the oxidation of *o*-diphenols to their corresponding *o*-quinones (monophenolase and diphenolase activities, respectively). The active site of TYR takes on three forms in the catalytic cycle:  $E_m$  (*met*-TYR,  $Cu^{2+}Cu^{2+}$ ),  $E_d$  (*deoxy*-TYR,  $Cu^{2+}Cu^{2+}$ ) and  $E_{ox}$  (*oxy*-TYR,  $Cu^{2+}Cu^{2+}O^{2-}$ ) (Solomon *et al.*, 1996). In the TYR structure from *Streptomyces castaneoglobisporus* (Matoba *et al.*, 2006), each copper atom of the active site of TYR is coordinated with three histidines (two joined equatorially and the other axially) (Matoba *et al.*, 2006). The  $E_{ox}$  form can act both on monophenols and *o*-diphenols, while the  $E_m$  form is only active on *o*-diphenols (Sanchez-Ferrer *et al.*, 1995).

The instability of the products formed by the action of TYR on monophenols and *o*-diphenols, the *o*-quinones, is responsible for the formation of  $H_2O_2$  in the melanin biosynthesis pathway (Munoz-Munoz *et al.*, 2009) and, at the same time, hinders the kinetic characterisation of these substrates (Rodriguez-Lopez *et al.*, 2000; Espin *et al.*, 2000). For this reason, and to obtain correct measurements of the initial velocity that would permit quantitative kinetic studies, we used a reductant (NADH or  $AH_2$ ) to prevent the evolution of these *o*-

quinones and so be able to characterize kinetically the action of this enzyme on *o*-diphenols using spectrophotometric methods. Moreover, *o*-quinones can react with nucleophilic reagents such as MBTH or thiols such as L-cysteine (Rodriguez-Lopez *et al.*, 1994; Peñalver *et al.*, 2002), which is useful for directing them towards an adduct with a given stoichiometry. Because oxygen acts as a substrate of the enzyme, an oxymetric method has also been used to measure the enzymatic activity of TYR on some substrates (Rodriguez-Lopez *et al.*, 1992).

Cooperativity is a widely studied process in enzymology (Monod *et al.*, 1965; Koshland *et al.*, 1966). At first it was thought that this phenomenon was exclusive to proteins or oligomeric enzymes such as haemoglobin, and binding equilibrium models were proposed to explain it — first the model proposed by Monod, Wyman and Changeaux and subsequently that of Koshland, Nemethy and Filmer (Monod *et al.*, 1965; Koshland *et al.*, 1966). However, it was subsequently demonstrated that also monomeric enzymes had a sigmoid kinetics — Rabin's model and, later, that proposed by Ferdinand (Rabin, 1967; Ferdinand, 1976). Among enzymes which have been shown to deviate from the hyperbolic kinetics models are phosphofructokinase (Atkinson & Walton, 1965), isocitrate dehydrogenase of yeast (Hathaway & Atkinson, 1963) and heart malate dehydrogenase (Wolfe & Neilands, 1956).

When extracted in a latent form, the TYR of some vegetal sources, such as grapes (*Vitis vinifera cv Airen*) or iceberg lettuce (*Lactuca sativa L.*) (Valero & Garcia-Carmona, 1992; Chazarra *et al.*, 2001), show negative or positive cooperativity when the initial velocity data are represented *vs.* the substrate concentration, deviating from the typical hyperbolic kinetics described for enzymes

✉ e-mail: canovasf@um.es

**Abbreviations:** see Table 1. *Species and concentrations:*  $[O_2]_0$ , initial oxygen concentration; D, diphenol;  $[D]_0$ , initial diphenol concentration; M, monophenol;  $[M]_0$ , initial monophenol concentration; E, enzyme (tyrosinase);  $[E]_0$ , initial concentration of enzyme;  $E_{ox}$ , oxy-tyrosinase;  $E_d$ , deoxy-tyrosinase;  $E_m$ , *met*-tyrosinase. *Kinetic parameters:*  $V_0^D$ , initial rate of tyrosinase acting on D;  $V_m^D$ , initial rate of tyrosinase acting on M;  $V_{max}^D$ , maximal rate of tyrosinase for D;  $V_{max}^M$ , maximal rate of tyrosinase for M;  $k_{cat}^D$ , catalytic constant of tyrosinase acting on D;  $k_{cat}^M$ , catalytic constant of tyrosinase acting on M;  $K_m^{D(P)}$ , apparent Michaelis constant of tyrosinase for D in the kinetically preferred pathway;  $K_m^{M(P)}$ , apparent Michaelis constant of tyrosinase for M in the kinetically preferred pathway;  $K_{m,D}^{O_2(P)}$ , apparent Michaelis constant for  $O_2$  in the diphenolase activity on the kinetically preferred pathway;  $K_{m,D}^{O_2(S)}$ , apparent Michaelis constant for  $O_2$  in the diphenolase activity on the slow pathway;  $K_{m,M}^{O_2(P)}$ , apparent Michaelis constant for  $O_2$  in the monophenolase activity on the kinetically preferred pathway;  $K_{m,M}^{O_2(S)}$ , apparent Michaelis constant for  $O_2$  in the monophenolase activity on the slow pathway.

type Michaelis–Menten. In a recent work (Munoz-Munoz *et al.*, 2010), our group found deviations from hyperbolic kinetics when the steady-state rate was represented *vs.* the concentration of the *o*-diphenolic substrate in the diphenolase activity of mushroom TYR, when working with the physiological substrates L-dopa, and its isomer D-dopa. In light of this, we suggested the existence of a kinetically preferred pathway and a slow pathway in the catalytic mechanism of TYR acting on *o*-diphenols. This translated into the appearance of inhibition by excess substrate when the steady state rate was represented *vs.* initial *o*-diphenolic substrate concentration and sigmoid curves when the initial velocity was represented *vs.* the concentration of oxygen. These deviations from the classical hyperbolic behaviour shown by TYR when the initial substrate concentration is varied are demonstrated in the diphenolase activity of TYR (Munoz-Munoz *et al.*, 2010). However, they do not appear in the monophenolase activity (Munoz-Munoz *et al.*, 2010). These findings can be explained kinetically if we accept that, in the case of diphenolase activity, the enzymatic system functions in the steady state, while, in the case of monophenolase activity, the system works in rapid equilibrium.

Recently, in a paper dealing with mushroom tyrosinase, Haghbeen *et al.* (2010), proposed that the enzyme showed a mixed type of cooperativity, that is, positive at low substrate concentrations and negative at high concentrations. This type of cooperativity has also been described in other enzymes such as bovine seminal ribonuclease (Piccoli *et al.*, 1988), and requires several substrate binding sites. However, recent studies on the structure of mushroom tyrosinase describe it a monomer (Wichers *et al.*, 1996; 2003).

In a previous work, we demonstrated the kinetic cooperativity of tyrosinase acting on the monophenol/*o*-diphenol pair, L-tyrosine/L-dopa, and its isomers D-

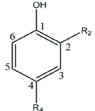
tyrosine/D-dopa (Munoz-Munoz *et al.*, 2010). Because the enzyme has wide substrate specificity, our aim in this work is to extend this kinetic study to different types of tyrosinase substrate in an attempt to generalise the applicable model. The substrates studied are characterised by their different groups in C-1: H in the case of catechol, a hydrophobic group like methyl (4-methylcatechol) or *tert*-butyl (4-*tert*-butylcatechol), a negatively charged group (3,4-dihydroxyphenylacetic acid) and 3,4-dihydroxyphenylpropionic acid), a positively charged group (dopamine and dopa methyl ester) and a doubly charged group, such as  $\alpha$ -methyl dopa and its respective monophenols. Moreover, the studied substrates were classified into three groups ( $S_A$ ,  $S_B$  and  $S_C$ ), according to the type of *o*-quinone that they generate when oxidised by TYR. The  $S_A$  group includes those that give rise to *o*-quinones that stabilise through a first order reaction, or which evolve through the attack of a nucleophile like MBTH in a first order reaction. The  $S_B$  group is formed of those that give rise to *o*-quinones that evolve with no clear stoichiometry, and lastly the  $S_C$  group comprises those that give rise to stable *o*-quinones. The analysis of the initial velocity data with regard to substrate concentration (monophenol, *o*-diphenol and oxygen) provides a general model that explains the cooperativity of TYR.

## MATERIALS AND METHODS

**Reagents.** Commercial mushroom tyrosinase (TYR) was purchased from Sigma (Madrid, Spain). The substrates (*o*-diphenols and monophenols) used in this work were: catechol (Cat), 4-*tert*-butylcatechol (TBC), 4-methylcatechol (4-MeCat),  $\alpha$ -methyl dopa, dopa methyl ester (DopaMeEster), dopamine, 3,4-dihydroxyphenylpropionic acid (DHPAA), 3,4-dihydroxyphenylacetic acid (DHPAA), phenol, 4-*tert*-butylphenol (TBF), *p*-cresol,  $\alpha$ -methyl tyrosine, tyrosine methyl ester, tyramine, 4-hydroxyphenylpropionic acid (PHPPA) and 4-hydroxyphenylacetic acid (PHPAA) and were purchased from Sigma-Aldrich. NADH and L-cysteine were also purchased from Sigma-Aldrich (Madrid, Spain). Other chemicals were of analytical grade and supplied by Merck (Darmstadt, Germany). Stock solutions of the diphenolic and monophenolic substrates were prepared in 0.15 mM phosphoric acid to prevent autooxidation. Milli-Q system (Millipore Corp.) ultrapure water was used throughout.

**Spectrophotometric assays.** These assays were carried out with a Perkin-Elmer Lambda-35 spectrophotometer, interfaced to a PC-computer, where the kinetic data were recorded, stored and later analyzed. The product of the enzyme reaction, the *o*-quinone, cannot be correctly detected experimentally due to the instability of *o*-quinones (Garcia-Carmona *et al.*, 1982; Garcia-Canovas *et al.*, 1982). Therefore, the reaction was followed in each case by measuring: (a) the disappearance of NsADH at 340 nm with  $\epsilon = 6230 \text{ M}^{-1} \cdot \text{cm}^{-1}$ , (Cat, 4-MeCat and TBC) (Garcia-Molina *et al.*,

**Table 1. Structures of substrates used in this work**

		
<i>o</i> -Diphenols	R <sub>4</sub>	R <sub>2</sub>
Catechol (Cat)	H	-OH
4-Methylcatechol (4MeCat)	CH <sub>3</sub>	-OH
4- <i>tert</i> -Butylcatechol (TBC)	-C-(CH <sub>3</sub> ) <sub>3</sub>	-OH
3,4-Dihydroxyphenylacetic acid (DHPAA)	-CH <sub>2</sub> -COO <sup>-</sup>	-OH
3,4-Dihydroxyphenylpropionic acid (DHPAA)	-CH <sub>2</sub> -CH <sub>2</sub> -COO <sup>-</sup>	-OH
Dopamine	-CH <sub>2</sub> -CH <sub>2</sub> -NH <sub>3</sub> <sup>+</sup>	-OH
Dopa methyl ester (DopaMeEster)	-CH <sub>2</sub> -CH(NH <sub>3</sub> <sup>+</sup> )-COOCH <sub>3</sub>	-OH
$\alpha$ -Methyl DOPA ( $\alpha$ -MeDOPA)	-CH <sub>2</sub> -C(CH <sub>3</sub> )(NH <sub>3</sub> <sup>+</sup> )-COO <sup>-</sup>	-OH
Monophenols	R <sub>4</sub>	R <sub>2</sub>
Phenol	-H	-H
<i>p</i> -Cresol	CH <sub>3</sub>	-H
4- <i>tert</i> -Butylphenol (TBF)	-C-(CH <sub>3</sub> ) <sub>3</sub>	-H
4-Hydroxyphenylacetic acid (PHPAA)	-CH <sub>2</sub> -COO <sup>-</sup>	-H
4-Hydroxyphenylpropionic acid (PHPPA)	-CH <sub>2</sub> -CH <sub>2</sub> -COO <sup>-</sup>	-H
L-Tyramine	-CH <sub>2</sub> -CH <sub>2</sub> -NH <sub>3</sub> <sup>+</sup>	-H
L-Tyrosine methyl ester	-CH <sub>2</sub> -CH(NH <sub>3</sub> <sup>+</sup> )-COOCH <sub>3</sub>	-H
$\alpha$ -Methyl-L-tyrosine	-CH <sub>2</sub> -C(CH <sub>3</sub> )(NH <sub>3</sub> <sup>+</sup> )-COO <sup>-</sup>	-H

2007), (b) the accumulation of dopachrome at 475 nm with  $\epsilon = 3600 \text{ M}^{-1} \cdot \text{cm}^{-1}$  ( $\alpha$ -methyl dopa, dopa methyl ester, tyrosine methyl ester,  $\alpha$ -methyl tyrosine) (Munoz *et al.*, 2006), (c) the appearance of the adduct between L-cysteine and *o*-diphenol at 300 nm with  $\epsilon = 2067, 2050$  and  $2007 \text{ M}^{-1} \cdot \text{cm}^{-1}$  for dopamine, DHPPA and DHPAA, respectively (Peñalver *et al.*, 2002) and (d) the appearance of the adduct between a nucleophile (MBTH) and the quinoneimine of 4-aminoanisole and 4-aminophenylalanine (Rodriguez-Lopez *et al.* 1994). The cuvette (final volume 1 ml) contained 30 mM sodium phosphate buffer (pH 7.0). The initial substrate (monophenol and *o*-diphenol) and oxygen concentrations were varied as indicated in the figure legends. The reaction was started by adding enzyme.

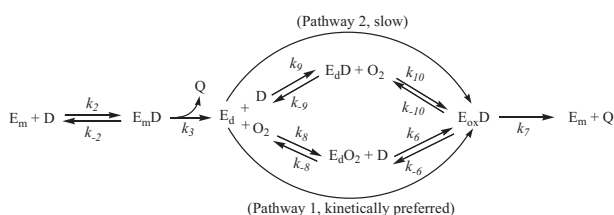
**Oxymetric assays.** Measurements of dissolved oxygen concentration were made with a Hansatech (Kings Lynn, Norfolk, UK) oxygraph unit controlled by a PC. The oxygraph used a Clark-type silver/platinum electrode with a 12.5 mm teflon membrane. The sample was continuously stirred during the experiments and its temperature was maintained at 25°C. The zero oxygen level for calibration and experiments was obtained by bubbling oxygen-free nitrogen through the sample for at least 10 min (Rodriguez-Lopez *et al.*, 1992). The initial concentrations of the monophenols TBF, *p*-cresol, tyramine, PHPPA, PHPAA and oxygen were varied as indicated in the legends of the figures. The initial oxygen concentration was varied as indicated in the legends of figures.

**Kinetic data analysis.**  $V^M_0$  or  $V^D_0$  values were calculated from triplicate measurements at each oxygen and reducing substrate concentration. The fitting was carried out using the Sigma Plot 9.0 program for Windows (Jandel Scientific, 2006), obtaining  $V^M_{\text{max}}$  or  $V^D_{\text{max}}$ , respectively, and  $K^{M(P)}_m$  or  $K^{D(P)}_m$ , respectively, by non-linear regression to the Michaelis–Menten equation.

**$^{13}\text{C}$ -NMR assays.**  $^{13}\text{C}$ -NMR spectra of several substrates were obtained at pH = 7.0 in a Varian Unity spectrometer at 300 MHz, using  $^2\text{H}_2\text{O}$  as solvent for the substrates. Chemical displacement ( $\delta$ ) values were measured relative to those for tetramethylsilane ( $\delta = 0$ ). The maximum line breadth accepted in the  $^{13}\text{C}$ -NMR spectra was 0.06 Hz. Therefore, the maximum accepted error for each peak of the spectrum was  $\pm 0.03$  p.p.m.

## RESULTS AND DISCUSSION

Mushroom tyrosinase (EC 1.14.18.1) is an enzyme that catalyses two types of reaction, the hydroxylation of monophenols to *o*-diphenols (monophenolase activity)



**Scheme 1.** Kinetic mechanism proposed to explain the action of TYR on *o*-diphenols

$E_m$ , *met*-TYR;  $E_d$ , *deoxy*-TYR;  $E_{ox}$ , *oxy*-TYR; D, *o*-diphenol; Q, *o*-quinone;  $E_mD$ , *met*-TYR/*o*-diphenol complex;  $E_dD$ , *deoxy*-TYR/*o*-diphenol complex;  $E_dO_2$ , *deoxy*-TYR/oxygen complex;  $E_{ox}D$ , *oxy*-TYR/*o*-diphenol complex.

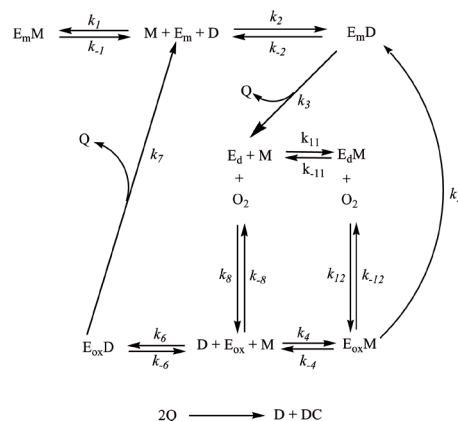
and the oxidation of *o*-diphenols to *o*-quinones (diphenolase activity) (Solomon *et al.*, 1996).

The activity on *o*-diphenols is described in Scheme 1, while the more complex activity on monophenols is described in Scheme 2. The product of monophenols and *o*-diphenols are *o*-quinones, which evolve chemically. As regards the evolution of these *o*-quinones, the substrates of the enzyme can be grouped into three types (groups  $S_A$ ,  $S_B$  and  $S_C$ ). The first group ( $S_A$ ) corresponds to substrates that originate *o*-quinones, which evolve to a stable product, either spontaneously through a first order reaction (such as L- $\alpha$ -MeDopa, DL- $\alpha$ -MeDopa, DopaMeEster or dopamine) or through attack by a nucleophilic reagent (pseudo first order reaction, as in the case of MBTH) towards a stable chromophore. In both cases an *o*-diphenol is accumulated in the medium. Group  $S_B$  comprises those substrates whose *o*-quinones do not evolve through a well defined stoichiometry so that *o*-diphenol is not accumulated quantitatively: for example, Cat/phenol and 4-MeCat/*p*-Cresol. Lastly, group  $S_C$  corresponds to those substrates that give rise to a stable *o*-quinone, such as the pair TBC/TBF.

## Monophenolase activity

The monophenolase activity is measured by adding the amount of *o*-diphenol at  $t=0$  that leads the system to reach the steady state, with  $[D]_0/[M]_0 = R = \text{constant}$  (Scheme 2) (Ros *et al.*, 1994).

**$S_A$  type substrates.** In the case of PHPPA, the chromophore obtained when MBTH reacts with the *o*-quinone was measured spectrophotometrically at the corresponding wavelength (Rodriguez-Lopez *et al.*, 1994). Figure 1 shows the data obtained by varying the initial concentration of PHPPA,  $[\text{PHPPA}]_0$ , and keeping the oxygen concentration fixed. In all cases a hyperbolic behaviour is observed. The only way in which the mechanism of Scheme 2 will behave hyperbolically, Eqn. (1) (Varon-Castellanos *et al.*, 1995), is to assume that the set of reactions occurs through rapid equilibrium, with the step controlled by  $k_5$  being limiting (Munoz-Munoz *et al.*, 2010). The expressions of  $\varphi_1$ – $\varphi_9$  and R are shown in the Appendix (at [www.actabp.pl](http://www.actabp.pl)).



**Scheme 2.** Kinetic mechanism proposed to explain the action of TYR on monophenols

$E_m$ , *met*-TYR;  $E_d$ , *deoxy*-TYR;  $E_{ox}$ , *oxy*-TYR; D, *o*-diphenol; Q, *o*-quinone; M, monophenol;  $E_mM$ , *met*-TYR/monophenol complex;  $E_mD$ , *met*-TYR/*o*-diphenol complex;  $E_dM$ , *deoxy*-TYR/monophenol complex;  $E_{ox}M$ , *oxy*-TYR/monophenol complex;  $E_dD$ , *oxy*-TYR/*o*-diphenol complex.

$$\frac{V_0^M}{[E]_0} = \frac{[\varphi_1 R [O_2]_0 + \varphi_2 R^2 [O_2]_0] [M]_0}{\varphi_3 R + [\varphi_4 + \varphi_6 R] [O_2]_0 + [\varphi_5 R + \varphi_7 [O_2]_0 + \varphi_8 R [O_2]_0 + \varphi_9 R^2 [O_2]_0] [M]_0} \quad (1)$$

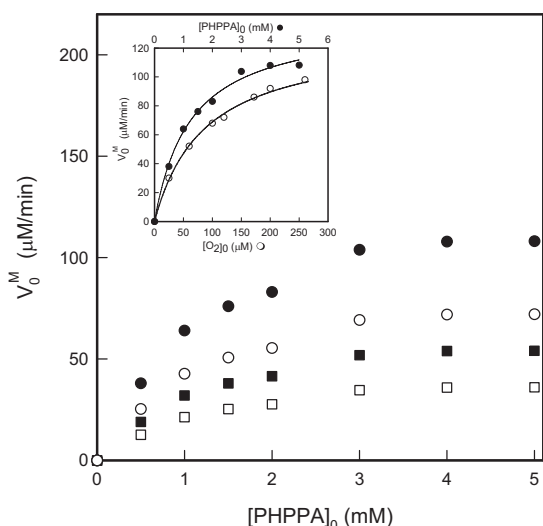


**Figure 1.** Initial velocities for the action of TYR versus different initial concentrations of PHPPA, at different concentrations of oxygen, determined by the appearance of MBTH-quinone adduct at  $\lambda = 474$  nm.

The experimental conditions were 30 mM sodium phosphate buffer (pH 7.0), 25 °C,  $[E]_0 = 30$  nM, the initial concentration of MBTH,  $[MBTH]_0$ , was 5 mM,  $[dimethyl\ formamide]_0 = 2\%$  (v/v) and the initial oxygen concentrations were (mM) (●) 260, (○) 120, (■) 60 and (□) 25. The PHPPA concentrations (mM) were varied as indicated in the figure, always adding a quantity of DHPPA for the DHPPA/PHPPA ratio (R) to remain constant ( $R = 0.093$ ). Inset. Representation of the initial velocity ( $V_0^M$ ) vs. initial concentration of  $O_2$ ,  $[O_2]_0$  (○) and the initial concentration of PHPPA,  $[PHPPA]_0$  (●).  $[PHPPA]_0$ - and  $[O_2]_0$ -values were 5 mM (○) and 260 mM (●), respectively. In both cases, the initial enzyme concentration was 30 nM.

Figure 1 Inset shows the values obtained for the initial velocity at different initial concentrations of oxygen,  $[O_2]_0$ , and at a saturating concentration of monophenol (initial monophenol concentration,  $[M]_0 \rightarrow \infty$ ). The hyperbolic behaviour confirms the rapid equilibrium described in Scheme 2. Non-linear regression analysis of the initial rate vs.  $[O_2]_0$  according to Eqn. (2), provides the value of  $K_{m,M}^{O_2(S)}$  (see Table 2).

$$V_0^M = \frac{V_{max}^M [O_2]_0}{K_{m,M}^{O_2(S)} + [O_2]_0} \quad (2)$$

Representation of the initial velocity values obtained at a saturating oxygen concentration vs. the concentra-

tion of monophenol and fitted to Eqn. (3) is shown in Fig. 1 Inset. Non-linear regression provides the value of  $K_m^{M(P)}$  (see Table 2).

$$V_0^M = \frac{V_{max}^M [M]_0}{K_m^{M(P)} + [M]_0} \quad (3)$$

The expressions  $K_m^{M(P)}$  and  $k_{cat}^M$  were developed in (Munoz-Munoz *et al.*, 2010). From Eqns. (4) and (5), we can obtain  $k_4$  and  $k_5$  (see Table 2).

$$K_m^{M(P)} = k_{cat}^M / k_4 \quad (4)$$

$$k_{cat}^M = k_5 \quad (5)$$

At monophenol concentrations where only the kinetic preferred pathway would be followed, an analytic expression can be obtained for the apparent Michaelis constant for oxygen in this pathway (Rodriguez-Lopez *et al.*, 1993), Eqn. (6). This constant cannot be determined from the experimental results because it is very small (Rodriguez-Lopez *et al.*, 1993), but can be calculated from Eqn. (6). The values obtained for the different monophenols studied in this paper are included in Table 2.

$$K_{m,M}^{O_2(P)} = \frac{3 k_{cat}^M}{2 k_8} \quad (6)$$

Another case of an  $S_A$  type monophenol, where the accumulated chromophoric product is measured directly, is that of L-tyrosine methyl ester — see Figs 2 and 2 Inset. Once again, the hyperbolic appearance of the initial velocity data represented *versus* the substrate concentration indicates that, kinetically, the mechanism occurs through rapid equilibrium. From these data, it is concluded that the Michaelis constant for oxygen in the slow pathway is greater than the apparent Michaelis constant in the preferred kinetic pathway, which is to be expected because, in the slow pathway, the monophenol binds to  $E_4$  before this enzymatic form binds oxygen (Table 2). This behaviour is seen again for the other  $S_A$  type substrates studied in this paper: tyramine,  $\alpha$ -methyl-L-tyrosine and PHPPAA.

**$S_B$  type substrates.** When this type of substrate is studied experimentally, oxymetric measuring techniques must be used, since the  $o$ -quinones evolve with no clear stoichiometry. Following the same methodology as de-

**Table 2.** Kinetic constants and parameters obtained for action of TYR on monophenols

Substrate	$K_m^{M(P)}$ (mM)	$K_{m,M}^{O_2(S)}$ ( $\mu$ M)	$K_{m,M}^{O_2(P)}$ ( $\mu$ M)	$k_{cat}^M$ ( $s^{-1}$ )	$k_4 \times 10^{-3}$ ( $M^{-1} \cdot s^{-1}$ )	$k_8 \times 10^{-7}$ ( $M^{-1} \cdot s^{-1}$ )	$\delta_4$ (p.p.m.)
Phenol	$0.61 \pm 0.04$	$63 \pm 5$	$0.47 \pm 0.04$	$10.8 \pm 1.5$	$17.71 \pm 1.95$	$2.3 \pm 0.4$	158.15
<i>p</i> -Cresol	$0.38 \pm 0.05$	$68 \pm 5$	$0.48 \pm 0.04$	$11.1 \pm 1.5$	$29.21 \pm 3.21$	$2.3 \pm 0.4$	155.50
TBF	$0.05 \pm 0.01$	$69 \pm 8$	$0.55 \pm 0.05$	$8.5 \pm 0.9$	$170.00 \pm 17.88$	$2.3 \pm 0.4$	156.10
PHPPAA	$1.72 \pm 0.23$	$90 \pm 10$	$2.03 \pm 0.18$	$46.8 \pm 1.8$	$27.21 \pm 3.52$	$2.3 \pm 0.4$	156.49
PHPPA	$0.41 \pm 0.07$	$74 \pm 6$	$2.74 \pm 0.21$	$63.2 \pm 2.3$	$154.15 \pm 17.12$	$2.3 \pm 0.4$	156.13
Tyramine	$0.62 \pm 0.16$	$45 \pm 5$	$1.18 \pm 0.21$	$27.3 \pm 3.2$	$44.03 \pm 4.58$	$2.3 \pm 0.4$	157.28
L-Tyrosine methyl ester	$0.51 \pm 0.11$	$44 \pm 2$	$0.16 \pm 0.02$	$3.7 \pm 0.1$	$7.25 \pm 0.81$	$2.3 \pm 0.4$	158.95
$\alpha$ -Methyl-L-tyrosine	$1.17 \pm 0.19$	$49 \pm 5$	$0.03 \pm 0.01$	$0.6 \pm 0.1$	$0.51 \pm 0.06$	$2.3 \pm 0.4$	159.10

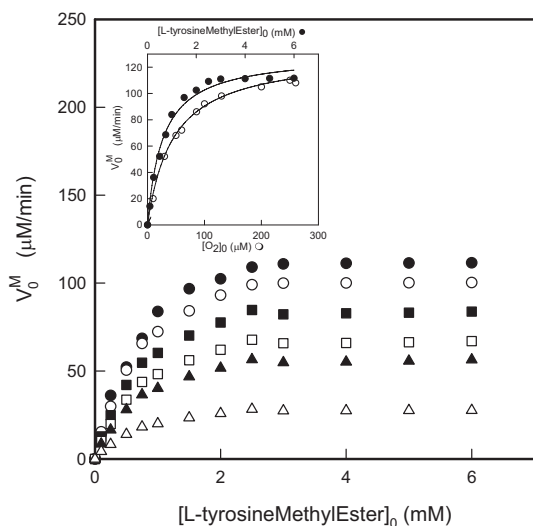


**Figure 2.** Initial velocities for the action of TYR versus different initial concentrations of tyrosine methyl ester, at different concentrations of oxygen, determined by the formation of amino-chrome

The experimental conditions were 30 mM sodium phosphate buffer (pH 7.0), 25 °C,  $\lambda=475$  nm,  $[E]_0=0.55$  mM and the initial oxygen concentrations were (mM) (●) 260, (○) 200, (■) 85 (□) 50, (▲) 30 and (Δ) 10. The tyrosine methyl ester concentrations (mM) were varied as indicated in the figure, adding, in each experiment, a concentration of dopa methyl ester, so that  $[D]_0/[M]_0=R=0.046$ . Inset. Representation of  $V_0^M$  vs  $[O_2]_0$  (○) and the initial concentration of tyrosine methyl ester,  $[tyrosine\ methyl\ ester]_0$  (●).  $[tyrosine\ methyl\ ester]_0$ - and  $[O_2]_0$ -values were 6 mM (○) and 260 mM (●), respectively. In both cases, the initial enzyme concentration was 0.55 mM.

scribed above, a quantity of *o*-diphenol proportional to the concentration of monophenol is added at  $t=0$ , so that the lag is eliminated and the initial velocity of the

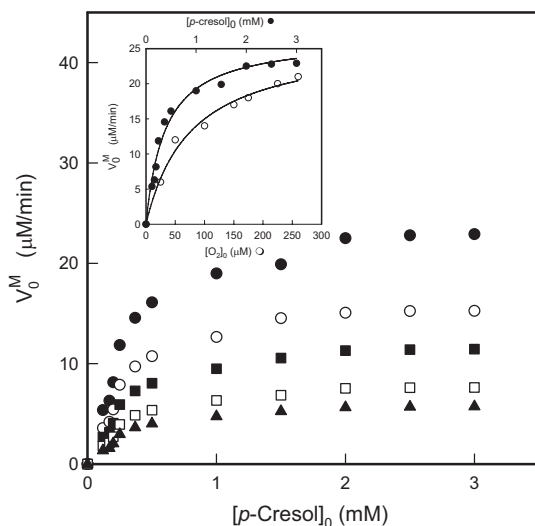


**Figure 3.** Initial velocities obtained for the action of TYR versus different initial concentrations of *p*-cresol, at different concentrations of oxygen, determined by the disappearance of molecular oxygen

The experimental conditions were 30 mM sodium phosphate buffer (pH 7.0), 25 °C,  $[E]_0=35$  nM and the initial oxygen concentrations were (mM) (●) 260, (○) 225, (■) 50, (□) 25 and (▲) 15. The *p*-cresol concentrations (mM) were varied as indicated in the figure, adding, in each experiment, a concentration of 4-MeCat, so that  $[D]_0/[M]_0=R=0.003$ . Inset. Representation of  $V_0^M$  vs.  $[O_2]_0$  (○) and the initial concentration of *p*-cresol,  $[p-Cresol]_0$  (●).  $[p-Cresol]_0$ - and  $[O_2]_0$ -values were 3 mM (○) and 260 mM (●), respectively. In both cases, the initial enzyme concentration was 35 nM.

steady-state can be measured correctly. In this way, phenol and *p*-cresol can be characterised (Figs. 3 and 3 Inset) (Table 2).

**$S_C$  type substrates.** Among the different monophenolic substrates of TYR studied, only TBF was found to provide a stable *o*-quinone. This was studied by adding at  $t=0$  a quantity of TBC that enabled the steady state to be reached with no lag period. The values of the kinetic constants are shown in Table 2.

### Diphenolase activity

The mechanism of diphenolase activity is straightforward and is described in Scheme 1. The pathway described (pathway 1, kinetically preferred) is the normal pathway followed by the enzyme. However, at high *o*-diphenol concentrations, the *deoxy*-tyrosinase form can bind to it before oxygen does to form a *deoxy*-tyrosinase/*o*-diphenol complex, which subsequently binds  $O_2$ , giving rise to a new form, *oxy*-tyrosinase/*o*-diphenol, which is transformed into *met*-tyrosinase and *o*-quinone (pathway 2, slow).

The kinetic characterisation of the *o*-diphenols is easier than in the case of monophenols, and several spectrophotometric methods have been described for the same (García-Molina *et al.*, 2007). Substrate types  $S_A$ ,  $S_B$  and  $S_C$  can be studied as indicated in the figures. Figure 4, for example, depicts the study of catechol (type  $S_B$ ) in the presence of NADH. The experimental results for the initial velocity obtained by varying the concentration of *o*-diphenol at different fixed concentrations of oxygen point to inhibition by excess of *o*-diphenol, suggesting that the system is working in a steady-state (Ferdinand, 1976). Note that the slow pathway begins earlier at low concentrations of oxygen. Figure 4 Inset shows the results obtained when the oxygen concentra-

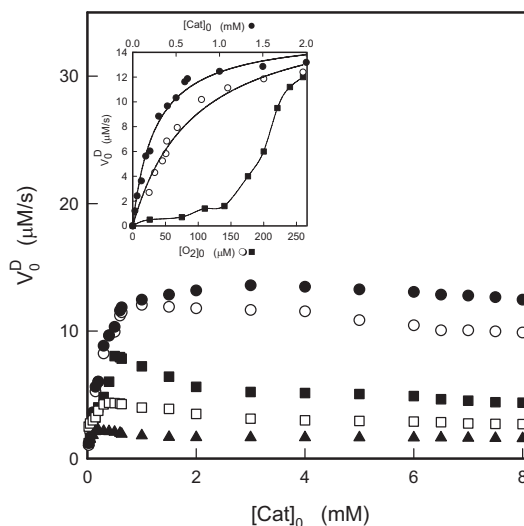


**Figure 4.** Initial velocities for the action of TYR versus different initial concentrations of Cat, at different concentrations of oxygen, determined by the disappearance of NADH

The experimental conditions were 30 mM sodium phosphate buffer (pH 7.0), 25 °C,  $\lambda=340$  nm, the initial concentration of NADH was 0.2 mM,  $[E]_0=10$  nM and the initial oxygen concentrations were (mM) (●) 260, (○) 200, (■) 50, (□) 35 and (▲) 25. The Cat concentrations (mM) were varied as indicated in the figure. Inset. Representation of the initial velocity ( $V_0^D$ ) vs.  $[O_2]_0$  (○, ■) and the initial concentration of Cat,  $[Cat]_0$  (●).  $[Cat]_0$  were 8 mM (○) and 2 mM (■) and  $[O_2]_0$  was 260 mM (●). In all cases, the initial enzyme concentration was 10 nM.

$$\frac{V_0^D}{[E]_0} = \frac{\beta_1[D]_0[O_2]_0 + \beta_2[D]_0[O_2]_0^2 + \beta_3[D]_0^2[O_2]_0}{\beta_4 + \beta_5[O_2]_0 + \beta_6[D]_0 + \beta_7[O_2]_0^2 + \beta_8[D]_0[O_2]_0 + \beta_9[D]_0^2 + \beta_{10}[D]_0[O_2]_0^2 + \beta_{11}[D]_0^2[O_2]_0} \quad (7)$$

tion is increased at a low concentration of *o*-diphenol — the sigmoid curve obtained indicates that the enzymatic system must work in the steady state (Ferdinand, 1976). Kinetic analysis of the mechanism described in Scheme 1 provides the corresponding velocity, Eqn. (7). The expressions of the parameters  $\beta_1$ – $\beta_{11}$  are described in the Appendix.

The data obtained at a saturating concentration of *o*-diphenol, when the reaction follows the slow pathway and in accordance with Eqn. (8), enables  $K_{m,D}^{O_2(S)}$  to be obtained (Fig. 4 Inset) (Table 3).

$$V_0^D = \frac{V_{\max}^D [O_2]_0}{K_{m,D}^{O_2(S)} + [O_2]_0} \quad (8)$$

with

$$K_{m,D}^{O_2(S)} = k_{cat}^D / k_{10} \quad (9)$$

From  $K_{m,D}^{O_2(S)}$  and in accordance with Eqn. (9),  $k_{10}$  can be calculated. Working at a saturating oxygen concentration, representation of the initial velocity *vs.* *o*-diphenol concentration (before the slow pathway of Scheme 2 is reached) provides  $K_m^{D(P)}$  with the help of Eqn. (10) (Fig. 4 Inset).

$$V_0^D = \frac{V_{\max}^D [D]_0}{K_m^{D(P)} + [D]_0} \quad (10)$$

with

$$K_m^{D(P)} = k_{cat}^D / k_6 \quad (11)$$

From  $K_m^{D(P)}$  and taking into account Eqn. (11),  $k_6$  can be calculated. The value of  $V_{\max}^D$  obtained with Eqn. (10) must be compared with the value obtained with Eqn. (8) since they should be the same (Figs. 4 Inset, 5 Inset, 6 Inset and 7 Inset).

Since there is no branching in the tyrosinase catalytic pathway (Scheme 1), the mechanism must follow the kinetic preferred pathway and it should be possible to obtain  $K_{m,D}^{O_2(P)}$ , Eqn. (12). From the value of  $k_8$  for the binding of oxygen to the form  $E_d$  (Rodríguez-López *et al.*, 2000), it is possible to obtain the values of this apparent constant (Table 3).

$$K_{m,D}^{O_2(P)} = k_{cat}^D / k_8 \quad (12)$$

Similar results were obtained with the rest of the *o*-diphenols studied. Figures 5 and 5 Inset show the results for DHPPA measured through the formation of an adduct with L-cysteine. The results obtained with TBC are depicted in Figs. 6 and 6 Inset, and the results obtained with DopaMeEster measuring the formation of aminochrome (Figs. 7 and 7 Inset).

### Slow step in the tyrosinase action mechanism

From the experimental data obtained for the monophenolase activity, Fig. 1–3, and for the diphenolase activity, Figs. 4–7, it can be assumed that the mechanism of Scheme 2 involves a much slower step than the others — the hydroxylation of monophenols to *o*-

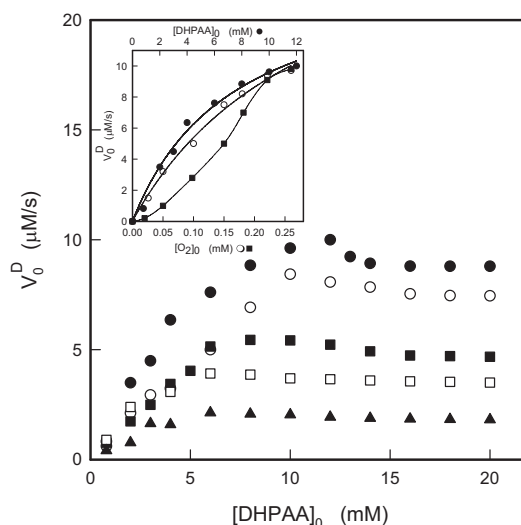


**Figure 5.** Initial velocities for the action of TYR versus different initial concentrations of DHPAA, at different concentrations of oxygen, determined by the formation of adduct between L-Cys and DHPPA

The experimental conditions were 30 mM sodium phosphate buffer (pH 7.0), 25 °C,  $\lambda=300$  nm, the initial concentration of L-Cys was 0.2 mM,  $[E]_0=0.7$  nM and the initial oxygen concentrations were (mM) (●) 260, (○) 220, (■) 100, (□) 75 and (▲) 40. The DHPPA concentrations (mM) were varied as indicated in the figure. Inset. Representation of  $V_0^D$  vs.  $[O_2]_0$  (○, ■) and the initial concentration of DHPPA,  $[DHPAA]_0$  (●) (○) were 20 mM (○) and 12 mM (■) and  $[O_2]_0$  was 260 mM (●). In all cases, the initial enzyme concentration was 0.7 nM.

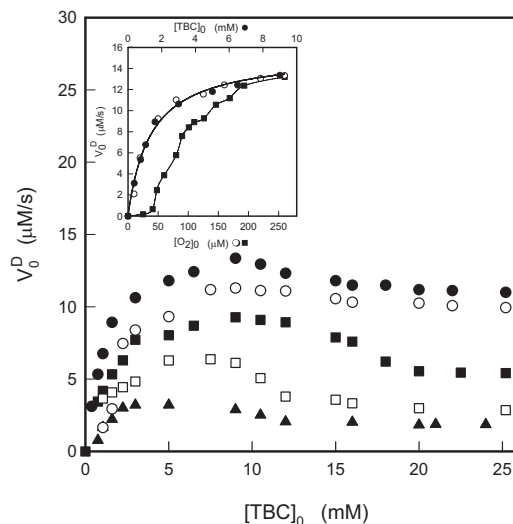


**Figure 6.** Initial velocities for the action of TYR versus different initial concentrations of TBC, at different concentrations of oxygen, determined by the disappearance of NADH

The experimental conditions were 30 mM sodium phosphate buffer (pH 7.0), 25 °C,  $\lambda=340$  nm,  $[NADH]_0=0.2$  mM,  $[E]_0=10$  nM and the initial oxygen concentrations were (mM) (●) 260, (○) 200, (■) 110, (□) 20 and (▲) 10. The TBC concentrations (mM) were varied as indicated in the figure. Inset. Representation of  $V_0^D$  vs  $[O_2]_0$  (○, ■) and the initial concentration of TBC,  $[TBC]_0$  (●) (○) were 26 mM (○) and 9 mM (■) and  $[O_2]_0$  was 260 mM (●). In all cases, the initial enzyme concentration was 10 nM.

diphenols governed by  $k_5$  (Eqn. 5). The system works in rapid equilibrium and hyperbolic behaviour is evident in the dependence of the initial velocity on the concentra-

**Table 3. Kinetic constants and parameters obtained for action of TYR on *o*-diphenols**

Substrate	$K_m^{D(P)}$ (mM)	$K_m^{O_2(S)}$ (mM)	$K_m^{O_2(P)}$ (mM)	$k_{cat}^D$ (s <sup>-1</sup> )	$k_6 \times 10^{-5}$ (M <sup>-1</sup> ·s <sup>-1</sup> )	$k_8 \times 10^{-7}$ (M <sup>-1</sup> ·s <sup>-1</sup> )	$k_{10} \times 10^{-6}$ (M <sup>-1</sup> ·s <sup>-1</sup> )	$\delta_4$ (p.p.m.)
Cat	0.15 ± 0.03	54 ± 5	37.82 ± 5.23	870.4 ± 46.1	58.00 ± 4.87	2.3 ± 0.4	16.11 ± 2.59	146.59
4-MeCAT	0.21 ± 0.03	59 ± 8	36.52 ± 5.47	840.2 ± 62.3	40.00 ± 3.56	2.3 ± 0.4	14.24 ± 2.81	144.06
TBC	1.50 ± 0.08	69 ± 7	28.04 ± 4.44	645.3 ± 58.2	4.30 ± 0.52	2.3 ± 0.4	9.98 ± 1.86	144.09
DHPAA	1.41 ± 0.18	100 ± 11	20.35 ± 3.35	468.4 ± 47.4	3.32 ± 0.41	2.3 ± 0.4	4.68 ± 0.85	144.96
DHPAA	0.83 ± 0.06	80 ± 9	27.17 ± 4.48	625.2 ± 63.3	7.53 ± 0.84	2.3 ± 0.4	7.81 ± 1.22	144.61
Dopamine	0.72 ± 0.08	90 ± 8	20.04 ± 3.43	461.1 ± 51.2	6.40 ± 0.69	2.3 ± 0.4	5.02 ± 1.06	145.58
DopaMeEster	0.85 ± 0.11	41 ± 4	19.13 ± 3.25	44.3 ± 4.8	0.52 ± 0.06	2.3 ± 0.4	1.07 ± 0.25	146.18
L- $\alpha$ MeDopa	5.21 ± 0.51	25 ± 3	1.78 ± 0.26	41.2 ± 3.2	0.08 ± 0.01	2.3 ± 0.4	1.64 ± 0.34	146.19
DL- $\alpha$ MeDopa	6.46 ± 0.58	28 ± 3	1.87 ± 0.27	43.1 ± 3.1	0.07 ± 0.01	2.3 ± 0.4	1.53 ± 0.29	146.19

tion of each of the substrates. However, in the diphenolase activity the oxidation of an *o*-diphenol occurs in the steady state, leading to the curves of Figs. 4–7, in agreement with Eqn. (7).

### Discussion of the kinetic constants depicted in Tables 2 and 3.

The values of the catalytic constants for the different monophenols (Table 2) are directly related to the power of the nucleophilic attack of the oxygen of the hydroxyl group of C-4, which is, in turn, directly related to the chemical shift  $\delta_4$ , as described previously (Espin *et al.*, 2000). A similar dependence is seen for the *o*-diphenols, but the nucleophilic power of the hydroxyl group of C-4 on the *o*-diphenols is greater than that of the hydroxyl group of C-4 on the monophenols, since  $\delta_4^D < \delta_4^M$ , so  $k_{cat}^D > k_{cat}^M$  (see Tables 2 and 3).

The constants that can be obtained from fitting the experimental data of the initial velocity *vs.* substrate

concentration are:  $K_m^{O_2(S)}$  at saturating concentrations of the substrate (monophenol or *o*-diphenol) and  $K_m^{D(P)}$  at saturating concentrations of oxygen (in the case of monophenols). For *o*-diphenols, the concentration of the *o*-diphenolic substrate would vary as long as the slow pathway is reached (zone of practically constant velocity in the curves), as seen from the Insets of Figs. 4–7. In this way,  $K_m^{D(P)}$  can be determined. These data are reflected in Tables 2 and 3, from which it can be seen that  $K_m^M \leq K_m^D$ . It can also be seen that the enzyme, in the  $E_d$  form, first binds to the monophenol or *o*-diphenol and then to oxygen, with a similar apparent Michaelis constant,  $K_m^{O_2(S)} \approx K_m^{O_2(S)D}$ .

If we consider that, experimentally, only the kinetically preferred pathway exists, the values of  $K_m^{O_2(P)}$  and  $K_m^{O_2(S)}$  can be obtained from the analytical expressions described previously, Eqns. (6) and (12) (Rodríguez-López *et al.*, 1993). These kinetic Michaelis constants (Tables 2 and 3) are much lower for monophenols than for *o*-diphenols. Moreover, both constants (for monophenols and *o*-diphenols) are lower than those obtained experimentally for the slow pathway.

The values of the binding constants of the substrates to the  $E_{ox}$  form ( $k_4$  for monophenols and  $k_6$  for *o*-diphenols) can be obtained from Eqns. (4) and (11), respectively. The *o*-diphenol binding constants governed by  $k_6$  are greater than those of monophenols governed by  $k_4$ , which agrees with the values of  $\delta_4$  (Tables 2 and 3).

The binding constants of oxygen to the enzyme could vary from the value of  $k_8$  (binding to  $E_d$  form) to the value of  $k_{10}$  (binding to  $E_dD$ ), as can be seen from Tables 2 and 3 ( $k_8 > k_{10}$ ). Note that the value of  $k_{10}$  (binding of oxygen to  $E_dD$ ) depends on the nature of the substrate, and is practically one order of magnitude greater for substrates with no charge, such as Cat, 4-MeCat and TBC.

Recently, allosteric cooperativity and cooperative inhibition have been described in mushroom tyrosinase (Hagheben *et al.*, 2010), as seen from a kinetic study and data analysis of both activities by means of Eadie-Hofstee graphs, using *p*-coumaric acid and 4-[(4-methylphenyl)azo]-phenol (MePAPh) as substrates for the monophenolase activity and caffeic acid and 4-[(4-methylphenyl)azo]-1,2-benzenediol (MePACat) for the diphenolase activity. The negative cooperativity in both activities observed by those authors was more pronounced in the case of monophenolase activity. The same authors suggest that other reports on the kinetics and inhibition of both activities of tyrosinase (Escribano *et al.*, 1989; Ros *et al.*, 1994; Park *et al.*, 2003; Yamazaki & Itoh, 2003; Fenoll *et al.*, 2004; Garcia-Molina *et al.*, 2005; Xue

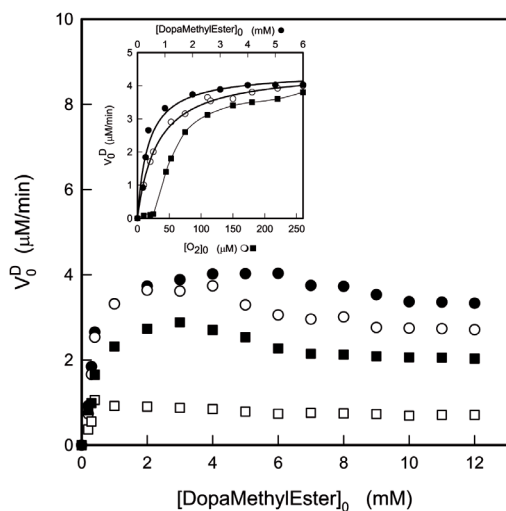


**Figure 7. Initial velocities for the action of TYR versus different initial concentrations of dopa methyl ester, at different concentrations of oxygen, determined by the formation of dopachrome.**

The experimental conditions were: 30 mM sodium phosphate buffer (pH 7.0), 25 °C,  $\lambda = 475$  nm,  $[E]_0 = 90$  nM and the initial oxygen concentrations were (mM): (●) 260, (○) 75, (■) 25 and (□) 10. The dopa methyl ester concentrations (mM) were varied as indicated in the figure. Inset. Representation of  $V_0$  vs  $[O_2]_0$  (○, ■) and the initial concentration of dopa methyl ester,  $[dopa\ methyl\ ester]_0$  (●).  $[dopa\ methyl\ ester]_0$  were 12 mM (○) and 5 mM (■) and  $[O_2]_0$  was 260 mM (●). In all cases, the initial enzyme concentration was 90 nM.

*et al.*, 2007) do not uncover the true kinetics due to the indirect methods and limited substrate concentrations used in the experiments (Haghbeen & Tan, 2003) and that a direct method, such as that involving the disappearance of substrate, should contribute to finding the true kinetics of the enzyme.

In a previous work (García-Molina *et al.*, 2007), we made a revision of the spectrophotometric methods used to follow the monophenolase and diphenolase activities of tyrosinase, using numerical integration to demonstrate that the rates of disappearance of substrate and appearance of product are equal when the system reaches the steady-state, even when the product that can be measured experimentally is accumulated after a series of chemical reactions. In the case of monophenolase activity, the system reaches the steady-state when a fixed quantity of *o*-diphenol has accumulated in the medium. In addition, we demonstrated that only the *o*-quinones (originating from the enzymatic conversion of monophenol or *o*-diphenol) that evolve with a given stoichiometry are capable of quantitatively accumulating *o*-diphenol in the medium. We also demonstrated that *o*-quinones are unstable and therefore can only be measured at short times. However, for diphenolase activity, Haghbeen *et al.* (2010) measured the disappearance of substrate over a period of five minutes (30 min in the case of monophenolase activity). We also demonstrated that monophenolase activity should be measured at different times, increasing as the monophenol concentrations increase. However, this was not taken into account by Haghbeen *et al.* (2010), who used a constant 30 min.

When measuring the disappearance of substrate in the ultraviolet region of the spectrum, it must be remembered that there is a danger of saturating the phototube of the spectrophotometer at high substrate concentrations. Although Haghbeen *et al.* (2010) used a 0.5 cm cuvette to be able to increase the substrate concentration, this is not sufficient to saturate the enzyme. Hence, in Fig. 2 (Haghbeen *et al.*, 2010), all the substrates were studied up to 100 mM regardless of the values of  $K_m$  described before (Haghbeen & Tan, 2003). The most striking case is the velocity *vs.* substrate concentration graph for *p*-coumaric acid (up to 100  $\mu$ M), for which the  $K_m$  is 97  $\mu$ M (Haghbeen & Tan, 2003). Later, the same authors increased the concentration to 200  $\mu$ M (Fig. 3) (Haghbeen *et al.*, 2010). Note that, according to Cleland (1967), substrate concentration should vary from  $K_m/5$  to  $5K_m$  to allow obtaining of correct parameters ( $V_{max}$  and  $K_m$ ). We must therefore conclude that the measurements made by Haghbeen and Tan (2003) and Haghbeen *et al.* (2010) are probably erroneous, which may be the origin of the deviations observed in monophenolase and diphenolase activities.

A wide variety of phenolic substrates of tyrosinase exist in plants, which explains why the enzyme is known as polyphenol oxidase. For example, the first six *o*-diphenols and their respective monophenols in Table 6 are found in a variety of plants. When the plants are attacked by predators such as bacteria, fungi or insects, the contact between the tyrosinases, their phenolic substrates and oxygen increases and the kinetic cooperativity of tyrosinase foments the formation of *o*-quinones and other melanogenes that are toxic for the predators' cells. Such kinetic cooperativity of tyrosinase therefore triggers an effective defence mechanism of the plants.

The three last substrates (mono- and *o*-diphenols) in Table 1 might be considered potential antitumor agents in the case of melanoma cells. The kinetic cooperativ-

ity of tyrosinase would increase the production of *o*-quinones and other melanogenes, and these could exit the melanosomes and interact with proteins and nucleic acids of the tumoral melanocytes, provoking oxidative stress, crosslinking reactions and the destruction of the melanin cells. A similar effect on melanoma cells has been demonstrated experimentally using derivatives of *bis*(catechol) as tyrosinase substrates (Bai *et al.*, 2010).

In conclusion, the experimental results obtained with a series of monophenol/*o*-diphenol pairs show that tyrosinase expresses kinetic cooperativity when it acts on *o*-diphenols (steady-state). However, during its action on monophenols, the cooperativity disappears due to the existence of a slow step, the hydroxylation of monophenols (rapid equilibrium).

## Acknowledgements

This paper was partially supported by grants from the Ministerio de Educación y Ciencia (Madrid, Spain) Project BIO2009-12956, from the Fundación Séneca (CARM, Murcia, Spain) Projects 08856/PI/08 and 08595/PI/08, from the Consejería de Educación (CARM, Murcia, Spain) BIO-BMC 06/01-0004 and FISCAM PI-2007/53 from the Consejería de Salud y Bienestar Social de la Junta de Comunidades de Castilla La Mancha. F.G.M. and J.L.M.M. have two fellowships from Fundación Caja Murcia (Murcia, Spain).

## REFERENCES

- Atkinson D, Walton GM (1965) Kinetics of regulatory enzymes. *Escherichia coli* phosphofructokinase. *J Biol Chem* **240**: 757–763.
- Bai M, Huang J, Zheng X, Song Z, Tang M, Mao W, Yuan L, Wu J, Weng X, Zou X (2010) Highly selective suppression of melanoma cells by inducible DNA cross-linking agents: bis(catechol) derivatives. *J Am Chem Soc* **132**: 15321–15327.
- Canovas FG, García-Carmona F, Sanchez JV, Pastor JL, Teruel JA (1982) The role of pH in the melanin biosynthesis pathway. *J Biol Chem* **257**: 8738–8744.
- Chazarra S, García-Carmona F, Cabanes J (2001) Hysteresis and positive cooperativity of Iceberg lettuce polyphenol oxidase. *Biochem Biophys Res Commun* **289**: 769–775.
- Cleland WW (1967) The statistical analysis of the enzyme kinetic data. *Adv Enzymol* **29**: 1–32.
- Escribano J, Tudela J, García-Carmona F, García-Canovas F (1989) A kinetic study of the suicide inactivation of an enzyme measured through coupling reactions-application to the suicide inactivation of tyrosinase. *Biochem J* **262**: 595–603.
- Espin JC, Varon R, Fenoll LG, Gilabert MA, García-Ruiz PA, Tudela J, García-Canovas F (2000) Kinetic characterization of the substrate specificity and mechanism of mushroom tyrosinase. *Eur J Biochem* **267**: 1270–1279.
- Ferdinand W (1976) In *The enzyme molecule*. Ferdinand W, ed, pp 139–185. John Wiley and Sons, London.
- García-Carmona F, García-Canovas F, Iborra JL, Lozano JA (1982) Kinetic study of the pathway of melanisation between L-dopa and dopachrome. *Biochim Biophys Acta* **717**: 124–131.
- García-Molina F, Muñoz JL, Varon R, Rodríguez-Lopez JN, García-Canovas F, Tudela J (2007) A review of spectrophotometric methods for measuring the monophenolase and diphenolase activities of tyrosinase. *J Agric Food Chem* **55**: 9739–9749.
- Haghbeen K, Tan EW (2003) Direct spectrophotometric assay of monooxygenase and oxidase activities of mushroom tyrosinase in the presence of synthetic and natural substrates. *Anal Biochem* **312**: 23–32.
- Haghbeen K, Khalili MB, Nematpour FS, Gheibi N, Fazli M, Alijanizadeh M, Jahromi SZ, Sariri R (2010) Surveying allosteric cooperativity and cooperative inhibition in mushroom tyrosinase. *J Food Biochem* **34**: 308–328.
- Hathaway JA, Atkinson DE (1963) The effect of adenylic acid on yeast nicotinamide adenine dinucleotide isocitrate dehydrogenase, a possible metabolic control mechanism. *J Biol Chem* **238**: 2875–2881.
- Jandel Scientific. Sigma Plot 9.0 for Windows™; Jandel Scientific: Core Madera 2006.

- Koshland Jr DE, Nemethy G, Filmer D (1966) Comparison of experimental binding data and theoretical models in protein containing subunits. *Biochemistry* **5**: 365–385.
- Matoba Y, Kumagai T, Yamamoto A, Yoshitsu H, Sugiyama M (2006) Crystallographic evidence that the dinuclear copper center of tyrosinase is flexible during the catalysis. *J Biol Chem* **281**: 8981–8990.
- Monod J, Wyman J, Changeaux JP (1965) On the nature of allosteric transitions: A plausible model. *J Mol Biol* **12**: 88–118.
- Munoz JL, Garcia-Molina F, Varon R, Rodriguez-Lopez JN, Garcia-Canovas F, Tudela J (2006) Calculating molar absorptivities for *o*-quinones: application to the measurement of tyrosinase activity. *Anal Biochem* **351**: 128–138.
- Munoz-Munoz JL, Garcia-Molina F, Varon R, Tudela J, Garcia-Canovas F, Rodriguez-Lopez JN (2009) Generation of hydrogen peroxide in the melanin biosynthesis pathway. *Biochim Biophys Acta* **1794**: 1017–1029.
- Munoz-Munoz JL, Garcia-Molina F, Varon R, Tudela J, Garcia-Canovas F, Rodriguez-Lopez JN (2010) New features of the steady-state rate related with the initial concentration of substrate in the diphenolase and monophenolase activities of tyrosinase. *J Math Chem* **48**: 347–362.
- Park Y, Jung J, Kim D, Kim W, Hahn M, Yang J (2003) Kinetic inactivation study of mushroom tyrosinase: Intermediate detection by denaturants. *J Protein Chem* **22**: 463–471.
- Peñalver MJ, Rodríguez-Lopez JN, García-Molina F, Garcia-Canovas F, Tudela J (2002) Method for the determination of molar absorptivities of thiol adducts formed from diphenolic substrates of polyphenol oxidase. *Anal Biochem* **309**: 180–185.
- Piccoli R, Di Donato A, D'Alessio G (1988) Co-operativity in seminal ribonuclease function. *Biochem J* **253**: 329–336.
- Rabin BR (1967) Co-operative effects in enzyme catalysis: A possible kinetic model based on substrate-induced conformation isomerisation. *Biochem J* **102**: 22c–23c.
- Rodriguez-Lopez JN, Ros-Martinez JR, Varon R, Garcia-Canovas F (1992) Calibration of a Clark-type electrode by tyrosinase-catalyzed oxidation of 4-tert-butylcatechol. *Anal Biochem* **202**: 356–360.
- Rodriguez-Lopez JN, Ros JR, Varon R, Garcia-Canovas F (1993) Oxygen Michaelis constants for tyrosinase. *Biochem J* **293**: 859–866.
- Rodriguez-Lopez JN, Escribano J, Garcia-Canovas F (1994) A continuous spectrophotometric method for the determination of monophenolase activity of tyrosinase using 3-methyl-2-benzothiazolinone hydrazone. *Anal Biochem* **216**: 205–212.
- Rodriguez-Lopez JN, Fenoll LG, Garcia-Ruiz PA, Varon R, Tudela J, Thorneley RNF, Garcia-Canovas F (2000) Stopped-flow and steady-state study of the diphenolase activity of mushroom tyrosinase. *Biochemistry* **39**: 10497–10506.
- Ros JR, Rodriguez-Lopez JN, Garcia-Canovas F (1994) Tyrosinase: kinetic analysis of the transient phase and the steady-state. *Biochim Biophys Acta* **1204**: 33–42.
- Sanchez-Ferrer A, Rodriguez-Lopez JN, Garcia-Canovas F, Garcia-Carmona F (1995) Tyrosinase: a comprehensive review of its mechanism. *Biochim Biophys Acta* **1247**: 1–11.
- Solomon EI, Sundaram UM, Machonkin TE (1996) Multicopper oxidases and oxygenases. *Chem Rev* **96**: 2563–2606.
- Valero E, Garcia-Carmona F (1992) Hysteresis and cooperative behavior of a latent plant polyphenoloxidase. *Plant Physiol* **98**: 774–776.
- Varon-Castellanos R, Garcia-Moreno M, Garcia-Sevilla F, Ruiz-Galea MM, Garcia-Canovas F (1995) *Computerized derivation of the steady-state equations of enzyme reactions*. A5, ed. Albacete, Spain
- Wichers HJ, Gerritsen YAM, Chapelon CGJ (1996) Tyrosinase isoforms from the fruit bodies of *Agaricus bisporus*. *Phytochemistry* **43**: 333–337.
- Wichers HJ, Recourt K, Hendriks M, Ebbelaar CEM, Biancone G, Hoerberichs FA, Mooibroek H, Soler-Rivas C (2003) Cloning, expression and characterisation of two tyrosinase cDNAs from *Agaricus bisporus*. *Appl Microbiol Biotechnol* **61**: 336–341.
- Wolfe RG, Neilands JB (1956) Some molecular kinetic properties of heart malic dehydrogenase. *J Biol Chem* **221**: 61–69.
- Xue CB, Wan-Chen L, Lin J, Xiang-Ye X, Ting X, Lei Y (2007) Inhibition kinetics of cabbage butterfly (*Pieris rapae* L.) larvae phenoloxidase activity by 3-hydroxy-4-methoxybenzaldehyde thiosemicarbazone. *Appl Biochem Biotechnol* **43**: 101–114.
- Yamazaki S, Itoh S (2003) Kinetic evaluation of phenolase activity of tyrosinase using simplified catalytic reaction system. *J Am Chem Soc* **125**: 13034–13035.